



NIH PUBLIC ACCESS

Author Manuscript

*Bioorg Med Chem Lett.* Author manuscript; available in PMC 2010 June 15.

Published in final edited form as:

*Bioorg Med Chem Lett.* 2009 June 15; 19(12): 3293–3296. doi:10.1016/j.bmcl.2009.04.077.

## Total synthesis and evaluation of 22-(3-azidobenzoyloxy)methyl epothilone C for photoaffinity labeling of $\beta$ -tubulin

Oliver E. Hutt<sup>a,c</sup>, Jun Inagaki<sup>a</sup>, Bollu S. Reddy<sup>a</sup>, Sajiv K. Nair<sup>a</sup>, Emily A. Reiff<sup>a</sup>, John T. Henri<sup>a</sup>, Jack F. Greiner<sup>a</sup>, David G. VanderVelde<sup>a</sup>, Ting-Lan Chiu<sup>c</sup>, Elizabeth A. Amin<sup>c</sup>, Richard H. Himes<sup>b</sup>, and Gunda I. Georg<sup>a,c,\*</sup>

<sup>a</sup> Department of Medicinal Chemistry, University of Kansas, 1251 Wescoe Hall Drive, Lawrence, KS 66045, USA

<sup>b</sup> Department of Molecular Bioscience, University of Kansas, 1200 Sunnyside Avenue, Lawrence, KS 66045, USA

<sup>c</sup> Department of Medicinal Chemistry, and Institute for Therapeutics Discovery and Development, University of Minnesota, 717 Delaware Street SE, Minneapolis, MN 55414, USA

### Abstract

The total synthesis of 22-(3-azidobenzoyloxy)methyl epothilone C is described as a potential photoaffinity probe to elucidate the  $\beta$ -tubulin binding site. A sequential Suzuki-aldol-Yamaguchi macrolactonization strategy was utilized employing a novel derivatized C1–C6 fragment. The C22-functionalized analog exhibited good activity in microtubule assembly assays, but cytotoxicity was significantly reduced. Molecular modeling simulations indicated that excessive steric bulk in the C22 position is accommodated by the large hydrophobic pocket of the binding site. Photoaffinity labeling studies were inconclusive suggesting non-specific labeling.

### Keywords

Epothilone; Photoaffinity labels; Microtubules

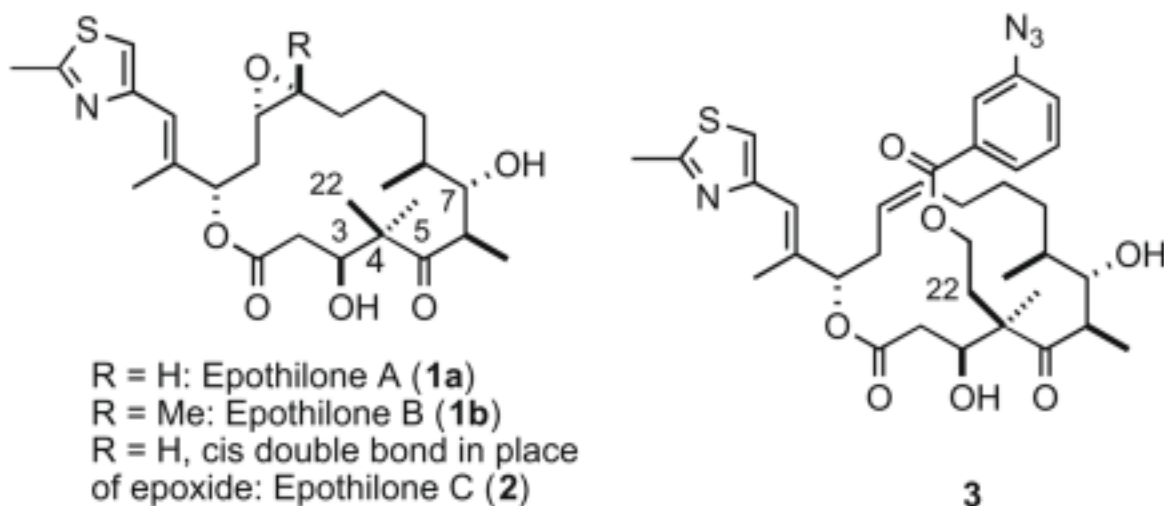
The epothilone class of natural products, typified by epothilone A (**1a**), epothilone B (**1b**), and epothilone C (**2**), is an extremely cytotoxic family of macrocyclic compounds. Their isolation from the myxobacterium *Sorangium cellulosum* was first reported in 1992 by Gerth et al.<sup>1</sup> It is well established that the binding sites on  $\beta$ -tubulin for the epothilones and taxanes overlap. However, early observations that the epothilones maintained toxicity against paclitaxel resistant cell lines, in which the resistance arose from tubulin point mutations in the paclitaxel binding site, suggested that the mode of binding was significantly different.<sup>2</sup> As a result, early attempts to find a shared pharmacophore between paclitaxel and epothilone B were unsuccessful.<sup>3–6</sup> The clinical importance<sup>7</sup> of this class of compounds has led to an explosion of synthetic activity<sup>8–10</sup> and a truly multi-disciplinary effort has culminated in two  $\beta$ -tubulin-epothilone binding models. The first model is based on combined molecular modeling, NMR,

\*Corresponding author. Professor and Department Head, Robert Vince Endowed Chair, McKnight Presidential Chair in Medicinal Chemistry, Department of Medicinal Chemistry Director, Institute for Therapeutics Discovery and Development, Room 452, College of Pharmacy, University of Minnesota, 717 Delaware Street SE, Minneapolis, MN 55414, USA. Tel.: +1 612 626 6320; fax: +1 612 626 6318. [georg239@umn.edu](mailto:georg239@umn.edu) (G.I. Georg).

**Publisher's Disclaimer:** This is a PDF file of an unedited manuscript that has been accepted for publication. As a service to our customers we are providing this early version of the manuscript. The manuscript will undergo copyediting, typesetting, and review of the resulting proof before it is published in its final citable form. Please note that during the production process errors may be discovered which could affect the content, and all legal disclaimers that apply to the journal pertain.

and electron-crystallography (EC) data of  $Zn^{2+}$  induced tubulin sheets,<sup>11</sup> while the second model is derived from NMR studies of epothilone bound to unpolymerized  $\alpha$ ,  $\beta$ -tubulin dimer in solution.<sup>12</sup>

In the EC-model the C7 hydroxyl, the C5 carbonyl, and the C3 hydroxyl of epothilone engage with Arg282 and Thr274 via H-bonds, while the C1 carbonyl interacts with Arg276. The thiazole ring then forms a hydrogen bond with His227 in the H7 helix. Although they are remote from the binding site, the residues Gln292 and Ala231 are important in maintaining the correct conformation of the M-loop and H7 helix, respectively.



The NMR-model supports the interaction between the C7 hydroxyl and Arg282 and Thr274 and further, that this interaction locks Arg276 into position to form a salt bridge with Asp224. The thiazole and His227 engage in a  $\pi$ - $\pi$  interaction and are not hydrogen bonded. Finally, and perhaps most intriguingly, is the involvement of the hydrophobic pocket hosting Phe270, which is vital for paclitaxel activity and also hosts the methyl group of epothilone B and thus accounts for its 10-fold increase in activity over epothilone A.

The underlying consensus of both the EC-model and NMR-model is a rigidification and alignment of the M-loop and the H7 helix, which leads to a conformational change in the  $\alpha$ ,  $\beta$ -tubulin dimer. This hypothesis is in agreement with a different overall macromolecular structure observed between polymerized and unpolymerized tubulin.<sup>13</sup>

Mammalian brain tubulin, the most abundant and studied of the tubulins, is highly heterogeneous due to the existence of seven  $\alpha$ - and eight  $\beta$ -isoforms and several types of post-translational modifications. These combinations are responsible for producing greater than 22 bands when mammalian brain tubulin is separated on high-resolution isoelectric focusing gels.<sup>14</sup> Given this complexity there still remains significant advances to be made in the understanding of microtubule stabilizing agents. Early information on the paclitaxel binding site was derived through photoaffinity labeling.<sup>15–20</sup> More recently discodermolide photoaffinity labeling studies have been reported.<sup>21</sup> However, to date the photolabeling with epothilone derivatives has remained elusive. Toward this end we have synthesized the C22-photoreactive derivative **3**. We now report the synthesis of **3** and the resulting microtubule assembly, cytotoxicity studies, and photoaffinity labeling studies.

The synthesis of the C22 analog follows the well precedented aldol/macrolactonization approach.<sup>22</sup> With the known aldehyde **12** in hand we focused our attention on the synthesis of

the modified C1–C7 fragment **11** (Scheme 1). Starting from the known  $\beta$ -hydroxy ester **4** two sequential Frater alkylations were carried out. Thus, the  $\beta$ -hydroxy ester **4** was treated with 2 equiv of LDA and the resulting dianion quenched with 1.1 equiv of allyl iodide to give the anti-allylated compound **5** in 82% yield. The procedure was subsequently repeated and quenched with MeI to provide the desired anti-methylated product **6** in 66% yield. The free alcohol was protected as the TBS ether (94%) and the alkene function of **6** was ozonolyzed to furnish aldehyde **7** (97%). The aldehyde was subsequently reduced and the resulting alcohol protected as the trityl ether.

The C6–C7 ethyl chain was then introduced by first converting the ester **8** to aldehyde **9** through a two-step reduction (80%)/oxidation (89%) sequence. The aldehyde **9** was then treated with EtMgBr and the resulting alcohol (71%) was oxidized to provide ketone **10** in 89% yield. Finally, the benzyl group was removed and the free primary C1 alcohol reprotected as TBS ether **11** in preparation for the aldol reaction.<sup>23</sup>

Accordingly, the C1–C7 fragment **11** was treated with LDA and then the aldehyde fragment **12** was added to give adduct **13** in 38% yield (Scheme 2). The newly formed alcohol function was protected as the TBS ether (90%) and the C1 primary TBS ether was removed (72%) subsequently. The resulting alcohol was sequentially oxidized to the aldehyde (98%) and then to the acid **14** (94%).

The TBS-protecting group on the allylic alcohol **14** was deprotected (96%) and the macrocycle closed by employing a Yamaguchi macrolactonization to form the core skeleton **15** in 77% yield. The trityl group was removed with CSA to give the corresponding primary hydroxyl derivative in 50% yield. Finally, the *meta*-azidobenzoic acid was converted to the acid chloride on treatment with oxalyl chloride, which was subsequently reacted with the epothilone derivative to form photoaffinity adduct **16** in 82%.<sup>24</sup> Removal of the TBS groups with TFA then gave the target compound **3** (Scheme 2).

The microtubule assembly properties and cytotoxicity of the *meta*-azido analog **3** are summarized in Table 1. In the microtubule assembly assay the photoaffinity analog **3** was found to assemble microtubules in a concentration-dependent fashion.<sup>25</sup> However, the assembly was not as rapid and did not reach the same extent as in the presence of epothilone B. Comparison of the ED<sub>50</sub> values shows that **3** is about 20% as effective as epothilone B. Compound **3** is much less potent against NCI-ADR and MCF-7 cancer cell lines. The very low cytotoxicity could be due to poor uptake of **3** by the cells.

The labeling studies, carried out on assembled microtubules with <sup>3</sup>H-*meta*-azido analog **3**, demonstrated that irradiation led to incorporation of label into the protein. However, competition studies showed that although 40  $\mu$ M epothilone B did not reduce the labeling by 10  $\mu$ M analog **3**, 40  $\mu$ M paclitaxel was able to displace approximately 50%. These data suggest that, although analog **3** can promote the assembly of microtubules, it might bind in such a way that it cannot be displaced by epothilone B or fully by paclitaxel. Another possibility is that **3** is displaced but when it is free in solution and irradiated, it produces reactive intermediates that react in a non-specific manner with the protein.

Given that we observed microtubule assembly with **3**, and that up to 50% of the binding was inhibited with Taxol, docking studies were conducted to probe tubulin binding modes and ligand–receptor interactions for analog **3**. Figure 1a shows the docked conformation of **3** in the  $\beta$ -tubulin binding site.<sup>11</sup> Figure 1b shows a comparison of the docked configurations of epothilone B (yellow) and analog **3** (cyan) in the  $\beta$ -tubulin active site. In analog **3**, the bulky 22-(3-azidobenzoyloxy)methyl group slightly reorients the hydrophobic C8–C15 portion of the compound to avoid unfavorable van der Waals interactions with the bulky C22 position. This relatively minor rearrangement does not significantly disrupt the hydrogen bonding

network between receptor and the C1–C7 portion of the ligand. However, in analog **3**, the thiazole hydrogen binds to Arg276 rather than to His 227 as is found with epothilone B.

In summary, the photoaffinity analog **3** promotes the assembly of tubulin into microtubules and the computer modeling studies revealed key ligand-receptor interactions. Specifically, molecular modeling simulations indicated that excessive steric bulk in the C22 position is adequately accommodated by the large hydrophobic pocket in the binding site. However, the non-specific covalent labeling limits the practical utility of this probe for further elucidation of the  $\beta$ -tubulin binding site.

## Acknowledgments

This work was supported by the National Institute of Health grants CA79641 and CA105305. E.A.R. and J.F.G. were supported by NIH Training Grant GM 07775. E.A.R. was also supported by DAMD 17-001-0303.

## References and notes

1. Gerth K, Bedorf N, Hoefle G, Irschik H, Reichenbach H. *J Antibiot* 1996;49:560. [PubMed: 8698639]
2. Gupta ML Jr, Bode CJ, Georg GI, Himes RH. *Proc Natl Acad Sci USA* 2003;100:6394. [PubMed: 12740436]
3. Wang M, Xia X, Kim Y, Hwang D, Jansen JM, Botta M, Liotta DC, Snyder JP. *Org Lett* 1999;1:43. [PubMed: 10822530]
4. Ojima I, Chakravarty S, Inoue T, Lin S, He L, Horwitz SB, Kuduk SD, Danishefsky SJ. *Proc Natl Acad Sci USA* 1999;96:4256. [PubMed: 10200249]
5. He L, Jagtap PG, Kingston DGI, Shen HJ, Orr GA, Horwitz SB. *Biochemistry* 2000;39:3972. [PubMed: 10747785]
6. Giannakakou P, Gussio R, Nogales E, Downing KH, Zaharevitz D, Bollbuck B, Poy G, Sackett D, Nicolaou KC, Fojo T. *Proc Natl Acad Sci USA* 2000;97:2904. [PubMed: 10688884]
7. Fojo T, Menefee M. *Ann Oncol* 2007;18:v3. [PubMed: 17656560]
8. Watkins EB, Chittiboyina Amar G, Jung J-C, Avery Mitchell A. *Curr Pharm Des* 2005;11:1615. [PubMed: 15892666]
9. Watkins EB, Chittiboyina AG, Avery MA. *Eur J Org Chem* 2006:4071.
10. Feyen F, Cachoux F, Gertsch J, Wartmann M, Altmann KH. *Acc Chem Res* 2008;41:21. [PubMed: 18159935]
11. Nettles JH, Li H, Cornett B, Krahn Joseph M, Snyder James P, Downing Kenneth H. *Science* 2004;305:866. [PubMed: 15297674]
12. Reese M, Sanchez-Pedregal VM, Kubicek K, Meiler J, Blommers MJJ, Griesinger C, Carlomagno T. *Angew Chem, Int Ed* 2007;46:1864.
13. Wang HW, Nogales E. *Nature* 2005;435:911. [PubMed: 15959508]
14. Williams RC, Shah C, Sackett D. *Anal Biochem* 1999;275:265. [PubMed: 10552916]
15. Loeb C, Combeau C, EhretSabatier L, BretonGilet A, Faucher D, Rousseau B, Commercon A, Goeldner M. *Biochemistry* 1997;36:3820. [PubMed: 9092811]
16. Combeau C, Commercon A, Mioskowski C, Rousseau B, Aubert F, Goeldner M. *Biochemistry* 1994;33:6676. [PubMed: 7911324]
17. Dasgupta D, Park H, Harriman GCB, Georg GI, Himes RH. *J Med Chem* 1994;37:2976. [PubMed: 7915327]
18. Rao S, Krauss NE, Heerding JM, Swindell CS, Ringel I, Orr GA, Horwitz SB. *J Biol Chem* 1994;269:3132. [PubMed: 7906266]
19. Rao S, Orr GA, Chaudhary AG, Kingston DGI, Horwitz SB. *J Biol Chem* 1995;270:20235. [PubMed: 7657589]
20. Rao S, He LF, Chakravarty S, Ojima I, Orr GA, Horwitz SB. *J Biol Chem* 1999;274:37990. [PubMed: 10608867]

21. Xia SJ, Kenesky CS, Rucker PV, Smith AB, Orr GA, Horwitz SB. *Biochemistry* 2006;45:11762. [PubMed: 17002277]
22. Balog A, Meng D, Kamenecka T, Bertinato P, Su DS, Sorensen EJ, Danishefsky SJ. *Angew Chem, Int Ed* 1997;35:2801.
23. C1–C7 fragment 11.  $^1\text{H}$  NMR (400 MHz,  $\text{CDCl}_3$ )  $\delta$  7.38–7.18 (m, 15H), 3.94–3.92 (m, 1H), 3.57–3.54 (m, 2H), 3.10–3.05 (m, 1H), 2.87–2.81 (m, 1H), 2.47–2.29 (m, 2H), 2.12–2.09 (m, 1H), 1.85–1.78 (m, 1H), 1.55–1.37 (m, 2H), 0.94 (s, 3H), 0.88–0.87 (m, 21H), 0.08–0.06 (m, 12H).  $^{13}\text{C}$  NMR (100 MHz,  $\text{CDCl}_3$ )  $\delta$  214.7, 144.3, 128.8, 128.5, 127.9, 127.0, 87.2, 73.9, 60.3, 59.9, 55.5, 37.5, 37.3, 32.4, 26.3, 26.1, 18.6, 18.4, 14.8, 7.6, –3.5, –3.6, –5.1. HRMS  $m/z$  calcd for  $\text{C}_{41}\text{H}_{66}\text{NO}_4\text{Si}_2$  (M +  $\text{NH}_4$ ) 692.4530, found 692.4538.  $[\alpha]_{\text{D}}^{22.5} - 17.5$  (c 2.55,  $\text{CHCl}_3$ ).
24. *Photoaffinity analog 3*:  $^1\text{H}$  NMR (400 MHz,  $\text{CDCl}_3$ )  $\delta$  7.75 (dm,  $J = 7.9$  Hz, 1H), 7.64 (t,  $J = 1.7$  Hz, 1H), 7.39 (t,  $J = 7.9$  Hz, 1H), 7.18 (dm,  $J = 8$  Hz, 1H), 6.98 (s, 1H), 6.58 (s, 1H), 5.38 (m, 2H), 5.34 (d,  $J = 9.9$  Hz, 1H), 4.37 (m, 2H), 4.20 (ddd,  $J = 11.2$  Hz,  $J = 9.5$  Hz, 5.7 Hz, 1H), 3.73 (d,  $J = 4.4$  Hz, 1H), 3.45 (br s, 1H), 3.18 (qd,  $J = 6.7$  Hz,  $J = 1.1$  Hz, 1H), 3.16 (s, 1H), 2.67 (m + s, 4H), 2.57 (dd,  $J = 14.9$  Hz,  $J = 11.5$  Hz, 1H), 2.41 (dd,  $J = 14.9$  Hz, 2.4 Hz, 1H), 2.35 (m, 1H), 2.28 (m, 1H), 2.16 (m, 2H), 2.08 (s, 3H), 1.54–1.8 (m, 4H), 1.23 (t,  $J = 7.2$  Hz, 2H), 1.21 (d,  $J = 6.9$  Hz, 3H), 1.16 (s, 3H), 1.00 (d,  $J = 7.1$  Hz, 3H).  $^{13}\text{C}$  NMR (125 MHz,  $\text{CDCl}_3$ ) 219.7, 170.2, 165.5, 165.1, 151.9, 140.7, 138.6, 133.4, 131.7, 129.9, 126.0, 125.2, 123.6, 119.9, 119.5, 115.9, 78.4, 73.9, 71.9, 61.9, 56.2, 41.6, 38.9, 38.6, 33.5, 32.5, 31.8, 30.7, 19.1, 15.9, 15.2, 14.2, 13.7, 13.1. IR (neat)  $\nu_{\text{max}}$  3515, 2358, 2115, 1724  $\text{cm}^{-1}$ . HRMS  $m/z$  calcd for  $\text{C}_{34}\text{H}_{44}\text{N}_4\text{O}_7\text{S}$  (M+H) 653.3009, found 653.2990.  $[\alpha]_{\text{D}}^{26} - 51.6$  (c 0.480,  $\text{CHCl}_3$ ).
25. Liu Y, Ali SM, Boge TC, Georg GI, Victory S, Zygmunt J, Marquez RT, Himes RH. *Comb Chem High Throughput Screening* 2002;5:39.
26. Barron DM, Chatterjee SK, Ravindra R, Roof R, Baloglu E, Kingston DG, Bane S. *Anal Biochem* 2003;315:49. [PubMed: 12672411]

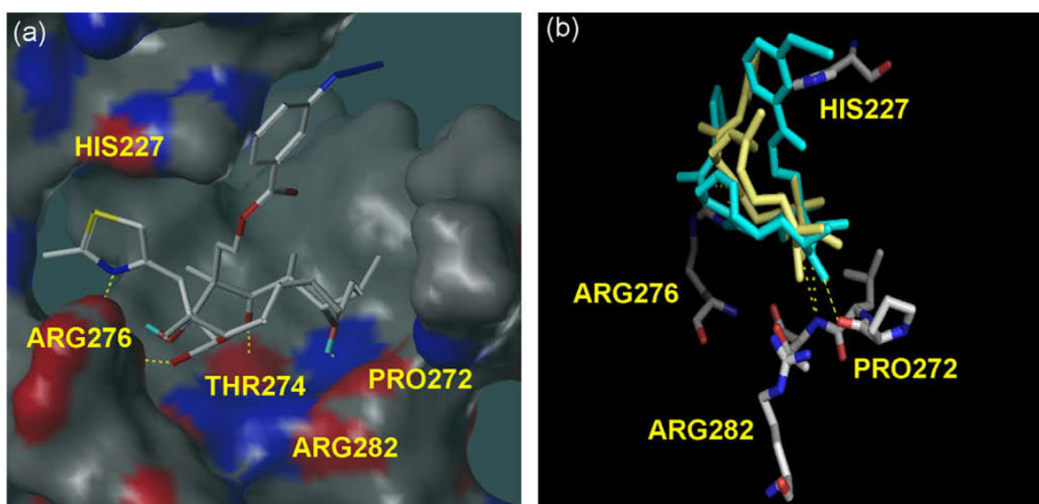
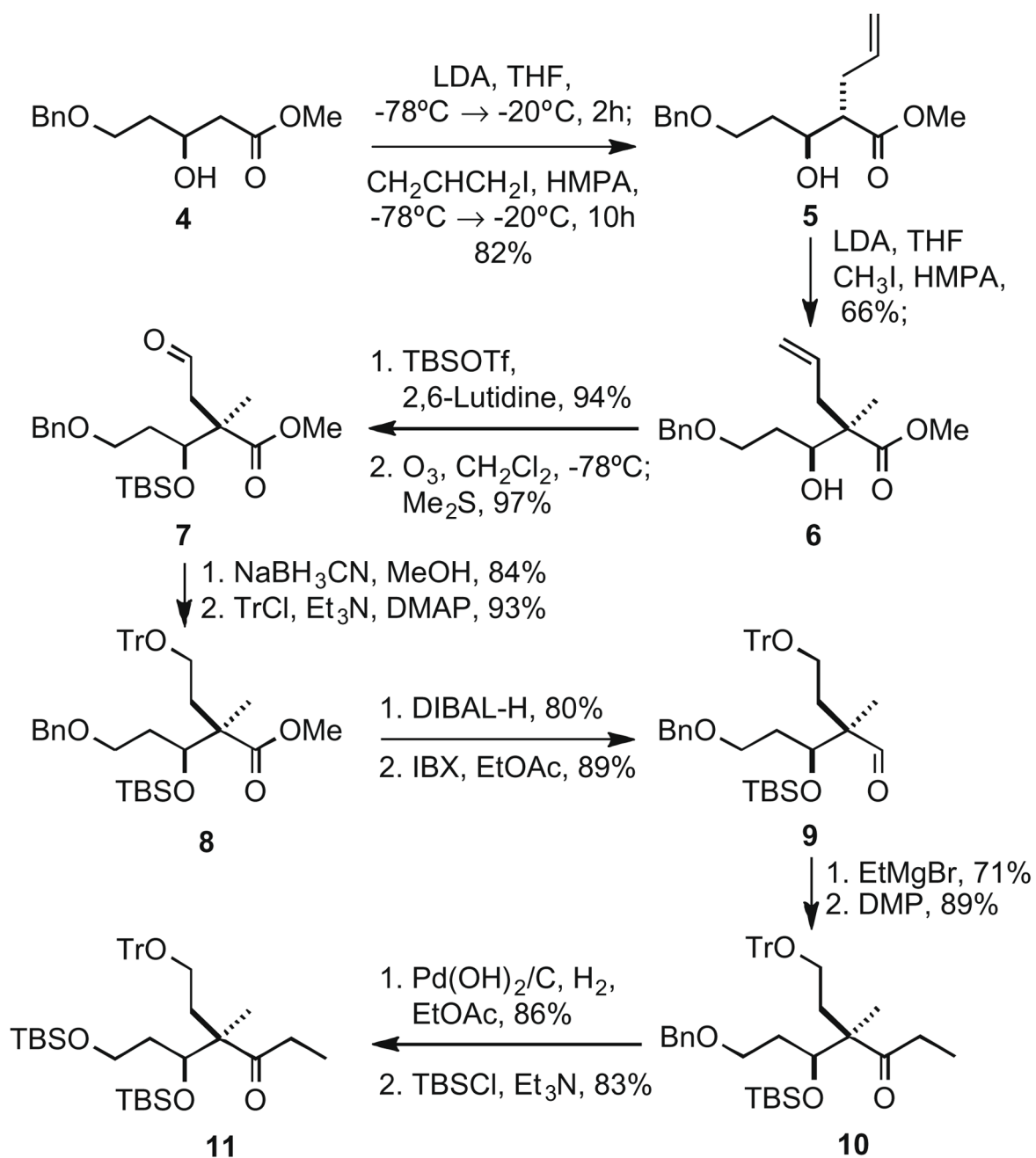
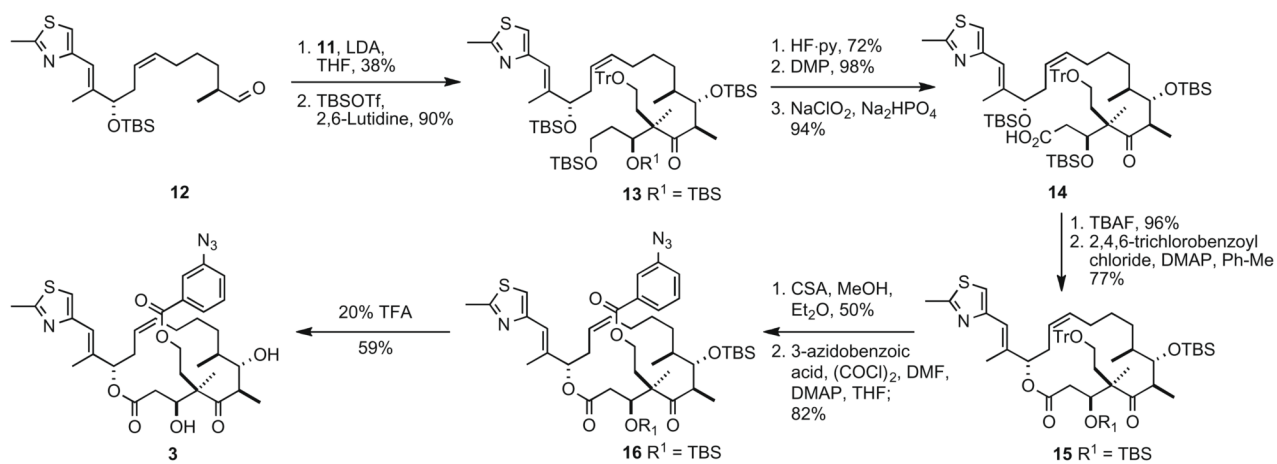


**Figure 1.**

(a) Docked configuration (Surflex-Dock, Tripos, Inc.) of 22-(3-azidobenzoyloxy)methyl epothilone C (**3**) shown with MOLCAD (Tripos, Inc.) electron density surfaces of the tubulin active site (1TVK11), onto which hydrogen bond donor and acceptor regions have been mapped. Red areas represent hydrogen bond donors; blue areas represent hydrogen bond acceptors; and gray indicates regions in which no hydrogen bonding takes place. Key ligand–receptor interactions are shown. Hydrogen bonding occurs between the thiazole nitrogen and one of the amino groups of Arg276; between the C1 carbonyl and the other amino group in Arg276; between the C5 carbonyl and the Thr274 backbone NH; and between the C7 OH and backbone carbonyl of Pro272. (b) The overlay of epothilone B (yellow) and **3** (cyan) in the binding site (PyMOL, 2006 DeLano Scientific LLC). Docking validation was carried out by comparing the docked configuration of EpoA to experiment (RMSD = 1.575 Å). The pre-docked conformation of **3** was prepared by modifying the experimental epothilone A structure and optimizing the resulting geometry using the MMFF94s force field in MOE (Chemical Computing Group, Inc.).



**Scheme 1.**  
Synthesis of C1–C7 fragment.



**Scheme 2.**  
Synthesis of arylazide epothilone analog **3**.



**Table 1**Biological testing of C22-epothilone photoaffinity analog **3**

Compounds	Microtubule assembly ED <sub>50</sub> , μM <sup>a</sup>	Cytotoxicity MCF-7 ED <sub>50</sub> , μM <sup>a,b</sup>	Cytotoxicity NCI-ADR ED <sub>50</sub> , μM <sup>a,b</sup>
Epothilone B	1.0	0.0015	0.0012
<b>3</b>	5.1 (5.1)	1.2 (632)	1.0 (833)

<sup>a</sup>ED<sub>50</sub> **3**/ED<sub>50</sub> epothilone B is in parenthesis.

<sup>b</sup>D<sub>50</sub> values for growth inhibition of human breast carcinoma cell line MCF-7. ED<sub>50</sub> values for growth inhibition of NCI-ADR, a P-glycoprotein over-expressing multi-drug resistant human ovarian carcinoma cell line. Cell proliferation assays were performed as previously described.<sup>25</sup> Microtubule assembly assays were performed as described in Ref.<sup>26</sup>.